

been found in the ion concentrations across the stream even with seeding flow rates ten times greater than those used with SF₆.

These results seem to indicate that when the argon plasma is seeded by very small amounts of SF₆ not only the electron density (as shown by the microwave measurements) but also the positive-ion density is markedly reduced. This conclusion is based on the fact that the double-probe saturation current is a measure of the ion density in the plasma and a simple replacement of electrons by negative ions should not radically change the probe saturation current. Even including the effect of the low mobility of heavy negative ions in the plasma, the very large changes in probe current that have been observed can only be explained by a reduction in the ion density. This suggests that the capture of electrons in the plasma by SF₆ to form negative ions is quickly fol-

lowed by a charge exchange process between the argon positive ions and the SF₆ negative ions. In addition, the efficiency of both these processes appears to be very high since the SF₆/A ratio is of the same order of magnitude as the ratio of electron to argon concentration in the unseeded plasma.

The authors wish to express their appreciation to Dr. M. P. Bachynski, for the many useful discussions concerning this investigation.

¹P. W. Huber, Proceedings of Plasma Sheath Symposium (Pergamon Press, New York, 1961), p. 172.

²W. M. Hickam and R. E. Fox, J. Chem. Phys. **25**, 642 (1956).

³E. O. Johnson and L. Malter, Phys. Rev. **80**, 58 (1950).

EXCITON-INDUCED IMAGES OF PHONON SPECTRA IN ULTRAVIOLET REFLECTANCE EDGES

J. C. Phillips*

Cavendish Laboratory, University of Cambridge, Cambridge, England

(Received 25 March 1963)

Ultraprecise measurements of the ultraviolet reflectance of a number of semiconductors have been reported by Lukeš and Schmidt.^{1,2} The relative accuracy of the reflectance is apparently 0.03% and of the spectral resolution 0.003 eV. Their results for Si at 359°K (Fig. 1) show a hyperfine splitting of the M₁ absorption edge at 3.350 eV into subsidiary edges at 3.310, 3.333, 3.367, 3.387, 3.404, 3.419, and 3.436 eV. Similar splittings which are seen in various absorption edges of other semiconductors are collected in Table I.

Here we observe that this structure is exactly what one expects when multiphonon transitions are taken into account. Consider first the direct transitions between conduction band *i* and valence band *j*. If we have an M₀ threshold at energy E₀, the form of the imaginary part of the dielectric constant ε₂ is³

$$\epsilon_2(\nu) = C(h\nu - E_0)^{1/2}, \tag{1}$$

while that of an M₁ edge⁴ at E₁ is

$$\epsilon_2(\nu) = C_1 - C_2(E_1 - h\nu)^{1/2} \quad h\nu \leq E_1, \tag{2}$$

$$= C_1 + C_3(h\nu - E_1) \quad h\nu \geq E_1. \tag{3}$$

The M₀ direct edge (1) is associated with a spheri-

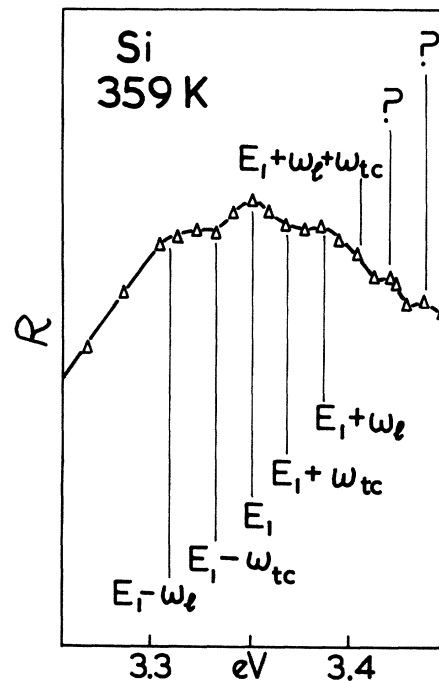


FIG. 1. Ultraviolet reflectance of Si near 3.35 eV at 359°K. The longitudinal acoustic phonon frequency is ω₁, the transverse acoustic ω_{1c}, and E₁ is the non-phonon intrinsic M₁ reflectance edge energy.

roidal neighborhood of k space defined by $(\hbar\delta k)^2 \leq m^*kT$. The M_1 direct edge (2)-(3) transitions occur along a hyperbolic surface⁵ in \vec{k} space defined by $E_i(\vec{k}) - E_j(\vec{k}) = E_1$.

Now consider transitions which involve the absorption or emission of n phonons, with $n=1$ for simplicity. These take place between states $E_i(\vec{k} + \vec{q}) - E_j(\vec{k}) = \hbar\nu \pm \hbar\omega_\alpha(\vec{q})$, where α is an index labeling phonon polarization. For M_0 edges these are called indirect transitions and they take place through virtual intermediate states which do not conserve energy.⁶ Usually $\delta k \ll q = |\vec{k}_i - \vec{k}_j|$ which means that $\hbar\omega_\alpha(\vec{q})$ takes on discrete values. Near an M_1 ultraviolet edge transitions may take place through energy-conserving intermediate states. Such transitions alter ϵ_2 by

$$\Delta\epsilon_2 = \sum_n \sum_{\vec{k}_i, \vec{q}_l, \alpha_l} \beta(\vec{q}_1, \alpha_1) \cdots \beta(\vec{q}_n, \alpha_n) \times [\epsilon_2(2\pi\nu \pm \omega_1 \cdots \pm \omega_n) - \epsilon_2(2\pi\nu)], \quad (4)$$

where $\sum \vec{q}_l = \vec{k}_i - \vec{k}_j$. In (4) $\beta(\vec{q})$ is an electron-phonon interaction constant proportional to $n(\vec{q}) + \frac{1}{2} \mp \frac{1}{2}$. Here $n(\vec{q})$ is the mean occupation number for phonons of energy $\hbar\omega_\alpha(\vec{q})$.

In the absence of detailed knowledge of the coupling constants β , we may assume that the surface covered by \vec{q}_l effectively samples the Brillouin zone. Then retaining only the terms $n = \pm 1$ for simplicity,

$$\Delta\epsilon_2 = \sum_\alpha B_\alpha \int d\omega_1 N_\alpha(\omega_1) [n(\omega_1) + \frac{1}{2} \mp \frac{1}{2}] [\epsilon_2(2\pi\nu \pm \omega_1) - \epsilon_2(2\pi\nu)], \quad (5)$$

where $N_\alpha(\omega)$ is the α th phonon density of states. At an M_1 edge $(d\epsilon_2/d\omega)_- = -\infty$, so that (5) maps the phonon spectrum $N_\alpha(\omega)$.

The density of phonon states $N_\alpha(\omega)$ in Ge and Si has been computed⁷ from neutron scattering measurements.^{8,9} The acoustic spectrum in Si is characterized by a large, narrow peak near 0.045 eV for the LA branch and a broad peak between 0.015 and 0.024 eV for the TA branch. In Fig. 2 we show $\epsilon_2(\omega)$ (direct transitions), $\epsilon_2(\omega) + \Delta\epsilon_2(\omega)$ when $N_1(\omega_1) = \delta(\omega_1 - 0.045 \text{ eV})$, and $\epsilon_2(\omega) + \Delta\epsilon_2(\omega)$ including N_1 and $N_2 = \text{const}$ for $0.015 \text{ eV} \leq \omega_2 \leq 0.024 \text{ eV}$. The latter curve bears a striking resemblance to the experimental curves of Fig. 1. Similar agreement is obtained for the other semiconductors where the phonon energies are half as great.

The structure at 3.404 eV in Fig. 1 may be due either to TO phonons or to the combination mode TA+LA. The edges at 3.419 and 3.436 eV are

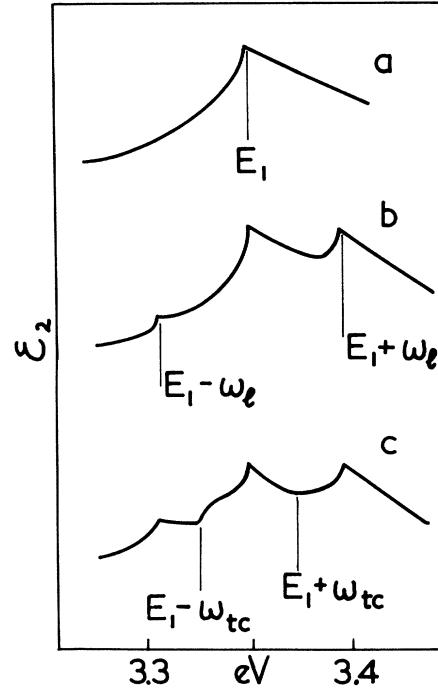


FIG. 2. The imaginary part of the dielectric constant ϵ_2 , as a function of energy near an M_1 edge at 3.35 eV. Curve a: no phonons; b: sharp longitudinal acoustic phonons; c: broad transverse acoustic phonons as well.

probably LA+2TA, LA+3TA. Multiphonon combination edges are also seen in other cases and are identified in Table I.

It is remarkable that the ultraviolet reflectance R displays¹⁰ the phonon spectrum with an accuracy comparable to that of superconductive tunneling.^{11,12} The similarity of this structure to theoretical expectations provides decisive confirmation of the ultraprecision claimed by Lukeš and Schmidt.

In ionic crystals energy-conserving electron-phonon absorption is conventionally described as exciton absorption with the electron and hole regarded as polarons.¹³ The localization of the electron and hole in the exciton state couples their Coulomb field to the phonon field. Cardona and Harbeke¹⁴ proposed that excitons were found at the M_1 edge in InSb and CdTe. This was criticized by Marple and Ehrenreich¹⁵ on the grounds that similar line shapes could be produced by interference from a nearby M_3 edge. The situation here is complicated by the possibility⁴ of additional singularities due to spin-orbit splitting ("pseudoexcitons," e.g., Table I, InAs, 2.45 eV).

It is important to realize that excitons near an

Table I. Hyperfine ultraviolet reflectance edges. The question marks label edges which are uncertain, usually because of sparsity of experimental measurements near that energy. In general, the phonon energies in the fourth column are consistent within 0.003 eV.

| Edge | Energy (eV) | Phonon modes (n, α) | Phonon energies (eV) | Edge | Energy (eV) | Phonon modes (n, α) | Phonon energies (eV) |
|--------|-------------|------------------------------|----------------------|-------|-------------|------------------------------|----------------------|
| M_1 | 3.350 | 0 | ... | | 2.560? | | 0.022 |
| Si | 3.310 | -LA | 0.040 | M_1 | 2.458 | 0 | ... |
| 359° | 3.333 | -TA | 0.017 | GaSb | 2.436 | -LA? | 0.022 |
| | 3.367 | +TA | 0.017 | 293° | 2.414 | -LO | 0.044 |
| | 3.387 | +LA | 0.037 | | 2.366 | -2LO | 2(0.046) |
| | 3.404 | +LA+TA | (0.037) + (0.017) | | 2.480 | LA? | 0.022 |
| | 3.419 | +LA+2TA? | (0.037) + 2(0.016) | | 2.502 | LO | 0.044 |
| | 3.436 | +LA+3TA? | (0.037) + 3(0.016) | | 2.524 | 3LA? | 3(0.022) |
| M_1 | 3.075 | 0 | ... | M_1 | 2.354 | 0 | ... |
| GaAs | 3.052 | -LA | 0.023 | InSb | 2.323 | -LO | 0.031 |
| 365° | 3.019 | -2LA? | (0.023) + (0.033) | 293° | 2.385 | +LO | 0.031 |
| | 3.099 | +LA | 0.022 | | 2.416 | +2LO | 2(0.031) |
| | 3.121 | +2LA | 2(0.022) | M_1 | 4.200 | 0 | ... |
| | 3.143 | +3LA? | 3(0.022) | GaSb | 4.192 | -TA | 0.008 |
| M_1 | 2.865 | 0? | ... | 297° | 4.180 | -LA | 0.020 |
| GaAs | 2.840 | -LA | 0.025 | | 4.172 | -LA-TA | 0.020 + 0.008 |
| 365° | 2.887 | +LA | 0.022 | | 4.160 | -2LA | 2(0.020) |
| | 2.909 | +2LA | 2(0.022) | | 4.208 | +TA | 0.008 |
| | 2.926 | +3LA? | 2(0.022) + 0.017 | | 4.220 | +LA | 0.020 |
| M_1 | 2.734 | 0 | ... | M_1 | 4.415 | 0 | ... |
| InAs | 2.712 | -LA? | 0.022 | Ge | 4.400 | -TA | 0.015 |
| 293° | 2.690 | -2LA | 2(0.022) | 297° | 4.391 | -LA | 0.024 |
| | 2.678 | -3LA? | 3(0.022) | | 4.382 | -TO | 0.033 |
| | 2.656 | -4LA | 4(0.022) | | 4.367 | -2LA | 2(0.024) |
| | 2.756 | +LA | (0.022) | | 4.358 | -LA-TO | 0.024 + 0.033 |
| | 2.778 | +2LA | 2(0.022) | | 4.334 | -2LA-TO | 2(0.024) + 0.033 |
| | 2.403 | | | | 4.430 | +TA | 0.015 |
| | 2.422 | | 0.019 | | 4.439 | +LA | 0.024 |
| | 2.437 | | 0.015 | | 4.455 | LA+TA | 0.024 + 0.016 |
| $M_3?$ | 2.497 | | | | 4.475 | 2LA+TA | 2(0.024) + 0.012 |
| InAs | 2.519 | | 0.022 | | 4.490 | 2LA+2TA | 2(0.024) + 2(0.015) |
| 293° | 2.538 | | 0.019 | | 4.514 | 3LA+2TA | 3(0.024) + 2(0.015) |

M_1 edge have a dynamical character qualitatively different from the conventional hydrogenic excitons formed near an M_0 edge. It is convenient to think of the periodic hyperboloidal energy surfaces in k space as undulating cylinders along the z axis. This is similar to a hydrogenic exciton with $m_z = \infty$. Compared to a conventional exciton binding energy $\epsilon_0 \sim 0.01$ eV, hyperboloidal or dynamically unstable exciton binding energies should be of order¹⁶

$$\epsilon_1 \sim 4\epsilon_0 \leq 0.1 \text{ eV.} \quad (6)$$

It has already been noted¹⁷ that at the 3.4-eV M_1 edge in Si, ϵ_2 has a large peak which is not of the expected character. The proposed explanation

for this peak required an energy-dependent line-width $\Gamma = 0.05$ eV for $E > 3.4$ eV and 0.02 eV for $E < 3.4$ eV. The conduction or valence intraband densities of states show no singularities, however. We conclude that this peak is caused by the singularity in the scattering density of states for dynamically unstable excitons.¹⁸ (The spontaneous emission part of β accounts for the asymmetry of Γ .) The fine structure shown in Fig. 1 provides conclusive proof for this interpretation.

For the 3.35-eV edge in Si, the magnitude of Γ or the strength of the $n = \pm 1$ edges compared to the $n = 0$ edge shows intermediate coupling ($\langle n \rangle \sim 1$) of the exciton to the phonon field. The coupling is even stronger ($\langle n \rangle \sim 4$) at the 4.3-eV edge in Si.

Such strong coupling is a consequence of the large volume of k space filled by the undulating cylinder $|E_i(\vec{k}) - E_j(\vec{k}) - E_1| \leq \epsilon_1$.

The phonon hyperfine structure appears to be unusually sensitive to changes in thickness of surface film. Lukeš and Schmidt¹ find that increasing the Ge film thickness from 37 Å to 48 Å enhances edges corresponding to $n=0, \pm 1$, but tends to suppress other edges. The bulk Ge absorption length here is 50 Å. This anomalous sensitivity may be due to spatial dispersion.¹⁹ Because excitons are formed, there are two normal modes of mixed photons and excitons for transverse electromagnetic waves. These are coherent, and their interference after reflection from the uneven bulk surface into the film affects the degree to which exciton-phonon hyperfine structure is observable in the external reflectance.

Dynamically unstable excitons, like hydrogenic excitons, may annihilate and emit photons and phonons. They may also emit photons and phonons by scattering, as hot electrons do. Finally, they may decay directly into free electrons and holes. We believe this to be the first positive identification of excitons which overlap the electron-hole scattering continuum.

*Guggenheim Fellow assisted by a Sloan grant on leave from the Department of Physics, University of Chicago, Chicago, Illinois.

¹F. Lukeš and E. Schmidt, Phys. Letters 2, 288 (1962): Ge, GaSb.

²F. Lukeš and E. Schmidt, 1962 Semiconductor Conference (Institute of Physics, London, 1962), p. 389: Si, InSb, InAs, GaAs.

³L. H. Hall, J. Bardeen, and F. J. Blatt, Phys. Rev. 95, 559 (1954).

⁴D. Brust, J. C. Phillips, and F. Bassani, Phys. Rev. Letters 9, 94 (1962).

⁵D. Brust (to be published), in which hyperbolic arcs obtained by sectioning these surfaces with symmetry planes are given.

⁶H. Y. Fan, Rept. Progr. Phys. 19, 114 (1956).

⁷J. C. Phillips, Phys. Rev. 113, 151 (1959).

⁸B. N. Brockhouse and P. K. Iyengar, Phys. Rev. 111, 747 (1958).

⁹B. N. Brockhouse, Phys. Rev. Letters 2, 256 (1959).

¹⁰We have discussed hyperfine structure in $\epsilon_2(\omega)$ whereas the measured structure occurs in the reflectance R . Whether the hyperfine structure in ϵ_2 will be reproduced in R depends on the relative variation of ϵ_1 and ϵ_2 near the M_1 edge. To see that no general statement can be made, it is sufficient to note that the phonon hyperfine structure is nearly absent² from $\Lambda_3(m_J = \frac{3}{2}) \rightarrow \Lambda_1$ but is quite evident in $\Lambda_3(m_J = \frac{1}{2}) \rightarrow \Lambda_1$. In the particular case of the M_1 edge shown in Fig. 1, one finds $(d\epsilon_2/d\epsilon_1)_- = 5$, while $(d\epsilon_2/d\epsilon_1)_+ = \frac{1}{2}$. This means that one-phonon absorption (-) hyperfine edges can appear larger than the corresponding emission (+) edge, and this is indeed seen to be the case.

¹¹J. M. Rowell, P. W. Anderson, and D. E. Thomas, Phys. Rev. Letters 10, 334 (1963).

¹²J. R. Schrieffer, D. J. Scalapino, and J. W. Wilkins, Phys. Rev. Letters 10, 336 (1963).

¹³Y. Toyozawa, Suppl. Progr. Theoret. Phys. (Kyoto) 12, 111 (1959).

¹⁴M. Cardona and G. Harbeke, Phys. Rev. Letters 8, 90 (1962).

¹⁵D. T. F. Marple and H. Ehrenreich, Phys. Rev. Letters 8, 87 (1962).

¹⁶M. A. Lampert, Phys. Rev. 97, 352 (1955).

¹⁷D. Brust, M. L. Cohen, and J. C. Phillips, Phys. Rev. Letters 9, 389 (1962).

¹⁸It is easy to see from phase-space arguments and the virial theorem that the effect of the real part of the electron-hole Coulomb self-energy $\Sigma_1(E)$ is to sharpen M_1 edges and blur M_2 edges. This may explain why no M_2 edges have yet been clearly resolved.

¹⁹S. I. Pekar, reference 2, p. 419.

SHAPE RESONANCES IN SUPERCONDUCTING THIN FILMS*

John M. Blatt and Colin J. Thompson

Courant Institute, New York University, New York, New York

and Applied Mathematics Department, University of New South Wales, Kensington, Australia

(Received 26 February 1963)

The basic equations for superconductors¹ are usually written for an infinite, homogeneous medium. We have set up the corresponding equations for a slab with thickness a , and solved them numerically for various slab thicknesses. The equations take into account, in a self-consistent fashion, the Coulomb potential generated by the charge density of the electrons plus an assumed uniform

background of positive charge. The boundary condition on the electron wave functions is that they vanish at the faces of the slab.

One rather expects resonance effects whenever an energy level $\eta_n(a)$, for motion perpendicular to the slab faces, passes through the Fermi surface as the thickness a is varied. What is surprising, however, is the size of the resonance ef-